THE JOURNAL OF PHYSICAL CHEMISTRY C

Article

pubs.acs.org/JPCC

Insights on Interfacial Structure, Dynamics, and Proton Transfer from Ultrafast Vibrational Sum Frequency Generation Spectroscopy of the Alumina(0001)/Water Interface

Aashish Tuladhar, Stefan M. Piontek, and Eric Borguet*

Department of Chemistry, Temple University, 1901 North 13th Street, Philadelphia, Pennsylvania 19122, United States

Supporting Information

ABSTRACT: Steady-state and time-resolved vibrational sum frequency generation (vSFG) were used to investigate the structure and dynamics of water at the α-$Al_2O_3(0001)$ surface. The vSFG spectra of the O—H stretch of water next to the $Al_2O_3(0001)$ surface are blue-shifted compared to the $Al_2O_3(11\bar{2}0)$ surface, indicating its weaker hydrogen bonding network. Consequently, the vibrational dynamics of the O—H stretch of the neutral $Al_2O_3(0001)$ surface is two times slower than the neutral $Al_2O_3(11\bar{2}0)$ surface. Furthermore, the vibrational dynamics of the O—H stretch of water next to charged Al_2O_3 surfaces is observed to be faster than that in bulk water and at charged SiO_2 surfaces, which could be due to (a) fast proton transfer dominating the vibrational relaxation and/or, (b) efficient coupling between the O—H stretch and the bend overtone via the presence of low frequency (~3000 cm^{-1}) O—H stretching modes. Lastly, the addition of excess ions (0.1 M NaCl) seems to have little to no effect on the time scale of vibrational dynamics, which is in contrast with the behavior observed at the silica surface, where addition of excess ions was observed to change the time scale of vibrational relaxation of interfacial water.

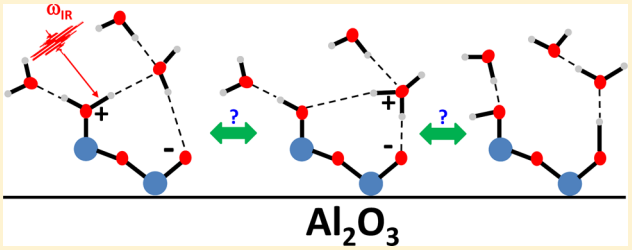

1. INTRODUCTION

Understanding how water interacts with mineral surfaces is of great significance in many geological, environmental, and technological processes, e.g., dissolution, corrosion, and heterogeneous catalysis.[1−3] Interactions between aqueous electrolyte solutions and the surface functional groups is unique to the mineral which gives rise to its distinctive pH dependent charging behavior. For instance, the point of zero charge (PZC) of silica[4,5] is ~pH 2, whereas the PZC is higher for alumina[6,7] (~pH 6−8). In order to completely comprehend the mechanisms and the time scales of interfacial chemistry at the mineral/water interface, it is critical to attain knowledge about the structure and dynamics of the aqueous environment next to the mineral surface.[3]

Nonlinear optical techniques such as second harmonic generation (SHG) and vSFG are excellent tools for investigating the mineral/water interface due to their interfacial selectivity.[4,5] Most SHG and vSFG studies have focused on investigating the silica/water or quartz/water interface.[4,5,8−16] The first vSFG spectrum of the silica/water interface was reported by the Shen group in 1994, when they successfully demonstrated the pH dependent charging behavior of the silica surface.[4] Many more theoretical[15,17−20] and experimental[8,10−12,14,16,21] investigations of mineral/water interfaces followed but most studies have been constrained to the neutral and negatively charged silica surface, where the interfacial water molecules are oriented with their OH pointing toward the interface.[21,22] The two peaks observed for the silica/water interface are near 3200 and 3400 cm^{-1} which are assigned to strongly and weakly hydrogen bonded O—H stretches of water, respectively.[4,8,13] However, this assignment is controversial mainly because the two peak structures observed at the air/water[23] interface and the silica/water[24] interface were argued to be due to strong inter- and intramolecular vibrational couplings (e.g., a Fermi resonance between the O—H stretch and the overtone of the water bend) as revealed by performing isotopically diluted (HOD in D_2O) experiments that allowed decoupling of the O—H stretching and water bending mode overtone.[24]

It was recently shown that the vibrational relaxation dynamics of the O—H stretch at the silica/water interface is slow (~570 fs) for the neutral silica surface, whereas at the negatively charged silica surface, the dynamics is much faster (~255 fs), similar to bulk water.[10] The latter result was shown to be a consequence of sampling of near interface (but bulk-like) water whose contribution can be screened in the presence of excess ions.[12] While there have been many studies involving the silica/water interface which have led to a better understanding of interfacial water next to silica surfaces, the inability to perform experiments at a positively charged surface means that a complete picture of interfacial water cannot be formulated.

Since the PZC of alumina is ~pH 6−8,[6,7] it provides an ideal opportunity to study and possibly distinguish between the structure and dynamics of water next to positively, neutral, and

Received: January 17, 2017
Published: February 24, 2017

DOI: 10.1021/acs.jpcc.7b00499
J. Phys. Chem. C 2017, 121, 5168−5177

negatively charged surfaces. Additionally, due to the high density of aluminol groups (similar to the surface density of water molecules),[25] the α-$Al_2O_3(0001)/H_2O$ interface provides the opportunity to detect surface aluminol groups and investigate how they affect the interfacial water chemistry.

The structure and ordering of water next to different alumina surfaces (e.g., 0001, $1\bar{1}02$, $11\bar{2}0$) has been investigated using theoretical[26−29] and experimental[3,6,30−37] techniques. Through X-ray reflectivity measurements,[3,37] Catalano showed that interfacial water next to the (0001) face of alumina is less "ordered" and more weakly hydrogen bonded compared to the $(11\bar{2}0)$ face. The Shen group investigated the $Al_2O_3(0001)/H_2O$[6] and the $Al_2O_3(11\bar{2}0)/H_2O$[32] interfaces using vSFG spectroscopy, which showed similar response except for the non-hydrogen bonded OH stretching region (i.e., the 3700 cm^{-1} peak was larger for the (0001) face). Another study showed that the initial surface preparation affected the vSFG spectra of the $Al_2O_3(0001)/H_2O$ interface. For example, the unetched rough $Al_2O_3(0001)$ surface showed a significantly larger 3700 cm^{-1} peak than the etched smooth surface.[38] In some but not all studies, a red-shifted peak ~3000 cm^{-1} was observed at various Al_2O_3/H_2O interfaces and assigned to hydrogen bonded surface aluminol groups.[30,31,35] Clearly, the structure and vibrational response of water next to the alumina surface is complex and still not completely understood.

Recently, we investigated the α-$Al_2O_3(11\bar{2}0)/H_2O$ using steady-state and time-resolved vSFG spectroscopy which revealed the presence of strongly hydrogen bonded species at ~3000 cm^{-1} which remained unperturbed in the presence of ions.[31] We assigned the 3000 cm^{-1} peak to the O−H stretch of strongly hydrogen bonded surface aluminol groups and/or interfacial water molecules that are strongly hydrogen bonded to the alumina surface, in agreement with our DFT calculations.[31] Additionally, the IR pump-vSFG probe measurements of the strongly hydrogen bonded O—H stretch region (3000−3300 cm^{-1}) revealed fast vibrational relaxation dynamics, which was insensitive to surface charge and ionic strength.[31]

The goal of the present study is to investigate the structure and the dynamics of interfacial water next to the $Al_2O_3(0001)$ surface using steady-state and time-resolved vSFG, to compare with our previous study of the $Al_2O_3(11\bar{2}0)$ surface and the fused silica surface and to test some of the predictions in the literature. The vSFG spectrum of the O—H stretch region of the $Al_2O_3(0001)/H_2O$ interface is blue-shifted and has less intensity around the 3000 cm^{-1} region compared to the $Al_2O_3(11\bar{2}0)/H_2O$ interface, indicating that the water next to the (0001) surface is in a weaker hydrogen bonding environment than the $(11\bar{2}0)$ surface as predicted by Catalano.[3,37] Moreover, the IR pump-vSFG probe experiments revealed that the vibrational dynamics of the strongly hydrogen bonded O—H stretch (2900−3300 cm^{-1}) at a charged alumina surface is faster than at the charged silica surface and even bulk water, which could be due to fast proton transfer reaction and/or more efficient coupling between the O—H stretch and the H_2O bend overtone via the presence of low frequency (red-shifted) OH species.

2. EXPERIMENTAL SECTION

2.1. Sample Preparation. α-Al_2O_3 triangular roof prisms (15 × 13 × 13 × 15 mm) with the 15 × 15 mm^2 face (opposite of the roof) cut at either the (0001) or the $(11\bar{2}0)$ orientation were purchased from Team Photon Inc. (San Diego, CA). Before the experiment, the α-Al_2O_3 triangular prisms were first cleaned with freshly prepared "piranha" solution (1 vol conc H_2O_2: 3 vol conc H_2SO_4) for ~30 min in a Teflon holder. (***CAUTION***: *"piranha is a very reactive mixture and must be handled with great care by using protective equipment—gloves, googles, and lab coat*). The prisms were then rinsed with copious amounts of deionized water (>18.2 MΩ·cm resistivity, Thermoscientific Barnstead Easypure II purification system with a UV lamp) and dried by filtered compressed N_2 gas. The prisms were then cleaned with low-pressure RF plasma for ~15 min, after which they were kept covered and allowed to equilibrate in ambient at room temperature before experiments. One of the prisms was coated with ~100 nm Au film and used for normalization of the raw data.

The triangular prism was mounted in a flow through sample holder. The acidic solutions were prepared by diluting as received concentrated HCl (Sigma-Aldrich, Trace SELECT grade) in deionized H_2O. Basic solutions were prepared by diluting as received NaOH solution (Fluka Analytical, analytical grade). The pHs of the solutions were verified with a pH-meter (Oakton).

2.2. Optical Setup. The one box Ti:sapphire oscillator + regenerative amplifier (Coherent, LIBRA−F-1K-110-HE+) produces 5.0 mJ at 800 nm with a pulse duration of 120 fs at a repetition rate of 1 kHz. 90% of 5 mJ (4.5 mJ) and is used to pump a commercial OPA (Coherent, TOPAS-Prime HE) to produce 1.3 W of signal and idler output. Tunable mid-infrared pulses are generated by collinear difference frequency generation (DFG) mixing of signal and idler pulses in an $AgGaS_2$ (AGS) crystal with typical pulse energy of 20 μJ @ 3 μm (~200 cm^{-1} fwhm). The mid-IR energy was divided, using a silicon wedge, to produce pump and probe IR pulses with the ratio of 3:1. The remaining 5% of the regenerative amplifier output, spectrally narrowed to a fwhm of ~2.5 nm using a narrow bandpass filter, is used as the visible light for SFG measurements. The IR pump (8 μJ/pulse), IR probe (3 μJ/pulse), and visible (5 μJ/pulse) beams incident at the surface with angles of 58°, 46°, and 51°, were focused to beam waists of ~75, ~75, and 200 μm, respectively. The visible incident angle was chosen to be greater than the critical angle (which was calculated to be ~50° for the 800 nm visible beam at Al_2O_3/H_2O interface using Snell's Law) to ensure enhancement of the vSFG signal via total internal reflection. All incident beams were p polarized. The p-polarized SFG signal was separated from the reflected visible light by a 750 nm short pass filter (Melles Griot) and was detected by a CCD detector (Princeton Instruments) coupled with a spectrograph (300i, Acton Research Corp.).

For steady-state vibrational SFG (vSFG), in order to cover the entire spectral region of the O—H stretching region (3000−3800 cm^{-1}), the phase matching angle for DFG in AGS crystal was adjusted to generate broader mid-IR output (covering 2800−3700 cm^{-1} region). The broadband mid-IR beam was spatially and temporally overlapped with the narrowband visible at the interface to produce SF photons. The raw vSFG spectrum from the Al_2O_3/H_2O sample was normalized with respect to the IR energy profile using a reference spectrum acquired from an α-Al_2O_3−Au sample.

One-color IR pump−vSFG probe was employed to study the vibrational relaxation dynamics of the O—H stretch at the $Al_2O_3(0001)/H_2O$ interface using narrower IR pulses (fwhm ≈ 200 cm^{-1}) were centered at 3100 cm^{-1}. Initially, the intense IR pump pulse transfers population from the vibrational ground

DOI: 10.1021/acs.jpcc.7b00499
J. Phys. Chem. C 2017, 121, 5168−5177

state ($\nu = 0$) to the first excited state ($\nu = 1$). The vSFG signal generated from the weaker probe IR and visible pulse monitors the ground-state population as a function of time. The position of the zero-time delay and the instrument response function were determined by the third-order cross-correlation ($\chi^{(3)}$) between the IR pump, IR probe, and visible. The time delay between the IR probe and the visible was fixed, and the IR pump beam delay was scanned with respect to the IR probe and visible for acquiring the $\chi^{(3)}$ and time-resolved vSFG measurements. The SFG was recorded in 33 fs time steps using custom written LabVIEW software. In order to account for the laser drift during typical scan time (15 min −1 h depending on the vSFG signal level which is sensitive to surface charge), an external shutter was placed in the pump IR path and at each time step pumped (shutter open) and unpumped (shutter closed) dynamics data were recorded. Then the pumped data was divided by the unpumped data to acquire normalized dynamics data. A typical pump−probe data (as shown later) is the average of 3−5 scans and each experiment was repeated 3−6 times on different days to generate error statistics.

3. RESULTS AND DISCUSSION

The normalized, Fresnel factor corrected vSFG spectra (Figure 1) of the O—H stretch region at the α-$Al_2O_3(0001)/H_2O$ interface at different bulk pH (2−12) revealed that the pH dependent charging behavior of the α-$Al_2O_3(0001)$ surface is consistent with the literature[6,7] and generally similar to our previously studied α-$Al_2O_3(11\bar{2}0)$ surface.[31] The vSFG spectra of the α-$Al_2O_3(0001)/H_2O$ interface are mainly comprised of two dominant peaks at 3200 and 3400 cm^{-1} in the hydrogen bonded O—H stretch region and a small peak at ~3720 cm^{-1} due to non- hydrogen bonded O—H stretches. At the charged alumina surface (pH 2, 4, 10, and 12), a shoulder around 3000 cm^{-1} (similar to the one observed in our previous study of the $Al_2O_3(11\bar{2}0)/H_2O$ interface[31]) is present which can be assigned to O—H stretches of strongly hydrogen bonded aluminol groups and/or interfacial water molecules. A recent MD simulation study[27] of a water film adsorbed on the α-$Al_2O_3(0001)$ surface revealed the presence of strongly hydrogen bonded (~3000 cm^{-1}) and non-hydrogen bonded (~3700 cm^{-1}) aluminol groups, which is in agreement with our assignment. Additionally, they also observed the presence of strongly, weakly, and non-hydrogen bonded molecularly adsorbed water (undissociated chemisorbed water) at the α-$Al_2O_3(0001)$ surface.[27] Clearly, the assignment of the vSFG spectra of the $Al_2O_3(0001)/H_2O$ interface is not straightforward as there are O—H stretches from both aluminol groups and interfacial water molecules.

The vSFG spectra of the O—H stretch region of the α-$Al_2O_3(0001)/H_2O$ interface are blue-shifted and have less intensity around the 3000 cm^{-1} region compared to the α-$Al_2O_3(11\bar{2}0)/H_2O$ interface (Figure 2). The blue-shift in the O—H stretch spectra is an indication of weaker hydrogen bonding environments experienced by the water molecules next to the $Al_2O_3(0001)$ surface compared to the $Al_2O_3(11\bar{2}0)$ surface, as predicted by Catalano's X-ray reflectivity measurements.[3,37] At the PZC (pH 6−8), the 3000 cm^{-1} species is absent (or tiny) at the $Al_2O_3(0001)/H_2O$ interface, whereas the shoulder around 3000 cm^{-1} region is still clearly visible for the $Al_2O_3(11\bar{2}0)/H_2O$ interface (Figure 2). The observed difference in amplitude of the 3000 cm^{-1} species at the (0001) and the $(11\bar{2}0)$ surface could be due to differences in surface termination between the two surfaces,[3,37] which could lead to

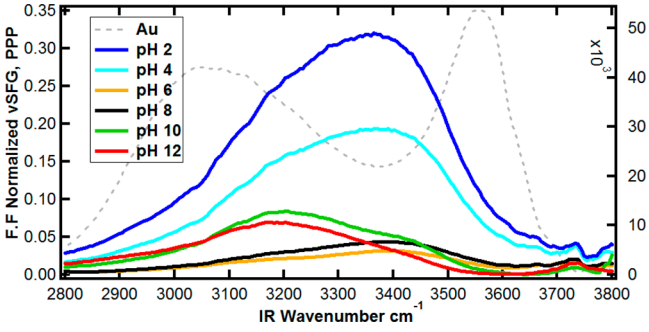

Figure 1. PPP-vSFG spectra of the α-$Al_2O_3(0001)/H_2O$ interface as a function of bulk pH (from 2−12). The gray dotted line represents the IR pulse profile acquired from the $Al_2O_3(0001)$−Au interface. All the data have been normalized with respect to the IR pulse profile and corrected for the wavelength dependence of the Fresnel factors, as has been described elsewhere.[31]

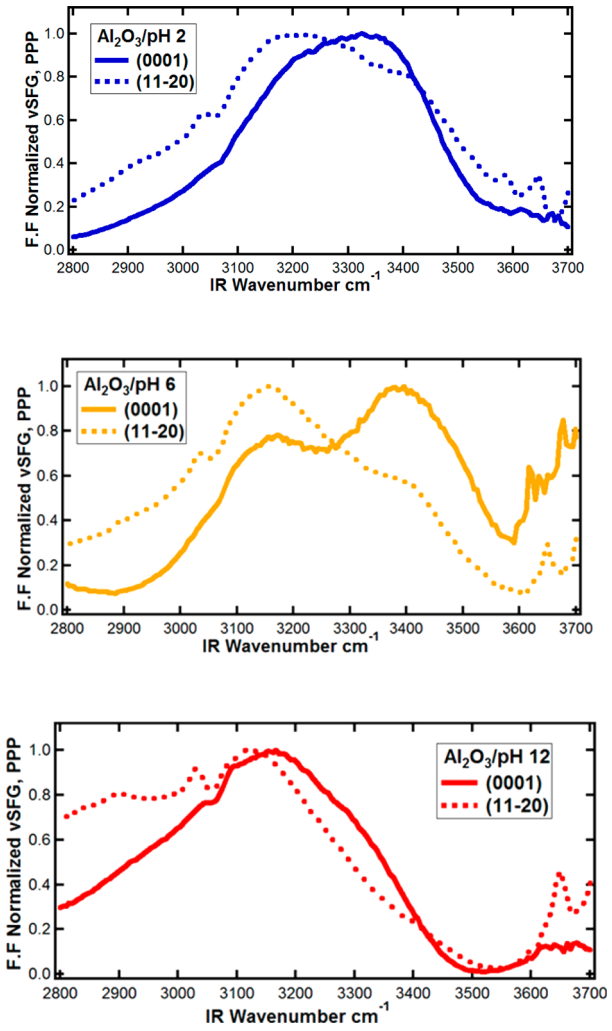

Figure 2. vSFG spectra of the α-$Al_2O_3(0001)/H_2O$ (solid lines) and the α-$Al_2O_3(11\bar{2}0)/H_2O$ interface (dotted lines) at bulk pH 2 (top, blue), pH 6 (middle, yellow), and pH 12 (bottom, red). All the data have been normalized with respect to the IR pulse profile and corrected for the wavelength dependence of the Fresnel factors, as described elsewhere.[31]

DOI: 10.1021/acs.jpcc.7b00499
J. Phys. Chem. C 2017, 121, 5168−5177

variations in the number and type of 3000 cm^{-1} species. This has important implications in the interpretation of the vibrational relaxation dynamics which will be discussed later. The vSFG signal in the non-hydrogen bonded region (>3600 cm^{-1}) for the two alumina surfaces is not reliable as the IR pulse energy is low, and the IR profile has some nonuniform shoulders in this region (gray dotted line in Figure 1). As a result, nonuniform shoulders are also present in the normalized vSFG spectra in the form of normalization artifacts. Therefore, we avoid interpreting the peaks or trends observed in the non-hydrogen bonded region in this study.

The red-shifted 3000 cm^{-1} O—H stretch is usually absent at the SiO_2/H_2O interface,[4,8,16] except in few studies at the quartz/water interface where a 3000 cm^{-1} peak with opposite phase (and presumably direction) compared to the interfacial water molecules was observed.[22,24] The difficulty in detecting surface silanol groups at the SiO_2/H_2O interface could be due to a lower density of Si—OH groups (~4 O—H groups/nm^2) compared to the density of water molecules at the surface (~20 H_2O/nm^2 based on bulk water density), i.e., for every single Si—OH group there are five HOH molecules at the interface.[39] Because the vSFG is proportional to the square of the number density, the signal arising from the interfacial water OH groups should be ~25 times greater than that from the surface silanol groups, all other factors being equal. In contrast, the density of OH groups due to surface aluminols is much higher (~13 OH groups/nm^2) at the α-Al_2O_3/H_2O interface,[25] which allows for its detection in the vSFG spectra.[31,35] We speculate that the absence or low density of hydrogen bonded surface OH groups at the SiO_2/H_2O interface and their presence at the α-Al_2O_3/H_2O interface directly affects the vibrational relaxation dynamics observed at each surface.

One-color IR pump−SFG probe experiments (described above in the Experimental Section) measuring the vibrational relaxation dynamics of the O—H stretch constitute another probe of the strength of the hydrogen bonding environment.[11,40−44] The vSFG probe continuously monitors the vibrational ground state (ν = 0) population of the O—H stretch and, at time zero, an intense pump IR pulse transfers population from the vibrational ground state (ν = 0) to the first excited state (ν = 1). As a result, bleaching (lowering) of the vSFG probe signal is observed. After the pump IR pulse has passed, the vSFG probe intensity starts to recover and the kinetics of this recovery directly reflects the vibrational lifetime of the excited O—H stretch.

In this study, the vibrational relaxation dynamics of the O—H stretch at the α-$Al_2O_3(0001)/H_2O$ interface at different bulk pH (Figure 3) was investigated. The four-level model (Figure S1−1, Supporting Information, SI) used for fitting is briefly described in the SI. The average time constants extracted from the fits to multiple experiments are summarized in Table 1. The effect of the IR pump power and the IR pump polarization on the ultrafast vibrational dynamics were also investigated (Figure S2−1,2) and both were observed to have negligible effect on the T_1 time scales.

Before discussing the vibrational relaxation dynamics of the O—H stretch at the $Al_2O_3(0001)/H_2O$ interface, it is important to briefly discuss bulk water and silica/water interface dynamics. The bulk liquid water dynamics has been extensively studied and the vibrational lifetime (T_1) is reported to be 190−260 fs.[45−47] The main mechanism of vibrational relaxation in bulk liquid water was reported to be via the Fermi resonance coupling between the overtone of the bending mode and the O—H stretch.[46,48−50] Additionally, the vibrational dynamics of ice and liquid water (deuterated, HOD:D_2O solution) have been investigated and the O—H stretch of ice was observed to relax two times faster than the liquid.[51] The faster relaxation in ice compared to liquid water can be explained with two distinct theories: (1) even though the number of hydrogen bonds between ice and liquid water is only marginally different, the ice structure is "more ordered" and is more strongly hydrogen bonded than liquid water, which provides a more efficient method of transferring vibrational energy to its surrounding environment; and (2) the O—H stretch of ice is red-shifted compared to liquid water,[13] and this allows for better coupling between the O—H stretch and the H_2O bend overtone, allowing the O—H stretch of ice to relax faster than in liquid water.

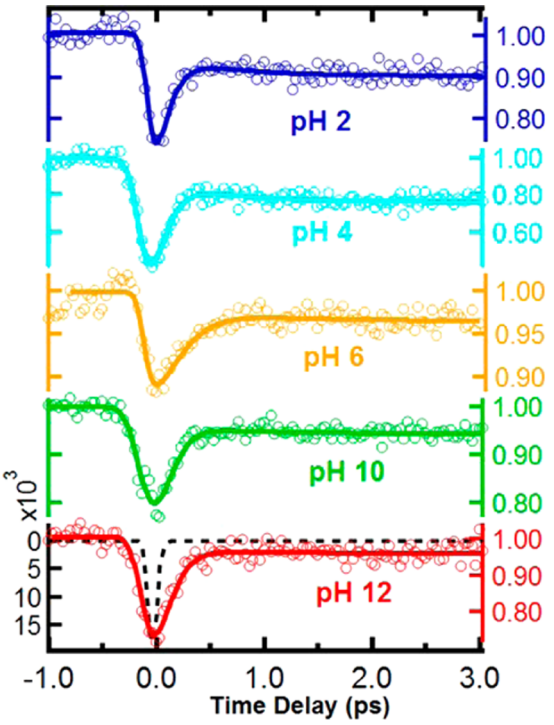

Figure 3. IR pump-vSFG probe vibrational dynamics of the interfacial OH species at the α-$Al_2O_3(0001)/H_2O$ interface for bulk pH 2, pH 4, pH 6, pH 10, and pH 12. The solid lines are the best fits consistent with a four-level system (described in the SI). The third-order cross-correlation between IR pump, IR probe, and visible is shown by the black dashed line and has a fwhm of ~105 fs, suggesting IR pulse durations of ~75 fs. P-polarized IR pump and PPP-polarized vSFG probe were used.

The vibrational relaxation of interfacial water next to a charged silica surface (pH = 6) was first reported to show that the interfacial water dynamics were similar to bulk water.[40] A subsequent study showed that the dynamics of water molecules next to the SiO_2 surface was sensitive to surface charge.[10] At pH 6, the observed results were consistent with the previous study, but at pH 2 (PZC of silica), the dynamics of water slowed down to ~570 fs.[10,12] This difference in behavior was explained in terms of changes in the relative surface charge at various pHs. At pH 6, where the silica surface is slightly negatively charged, an evanescently decaying surface electric field extends into the bulk water, orienting and/or polarizing the water molecules. As a result, a significant number of bulk water molecules exist in a noncentrosymmetric environment and

DOI: 10.1021/acs.jpcc.7b00499
J. Phys. Chem. C 2017, 121, 5168−5177

Table 1. T_1 and T_{th} Lifetime Extracted from Fitting Time-Resolved vSFG Data for α-Al_2O_3 (0001)/H_2O Interface for Bulk pH 2−12[a]

pH	2	4	6	10	12
T_1 (fs)	105 ± 16	125 ± 28	220 ± 19	103 ± 16	109 ± 10
T_{th} (fs)	632 ± 82	620 ± 75	610 ± 94	563 ± 108	595 ± 91

[a]Error bars are the standard deviation of the results of 3-6 independent experiments for each pH value.

contribute to the vSFG signal. Hence, bulk-like response dominated the vibrational dynamics at negatively charged silica surfaces (in the absence of excess ions). At pH 2, where the silica surface has a net zero charge, only the water at the interface contributed to the SFG signal and showed slow vibrational dynamics since the interfacial water molecules are incompletely solvated and cannot efficiently transfer energy. Therefore, interfacial water next to the neutral SiO_2 surface was shown to be fundamentally different from bulk water.[10]

Further experiments observed slowing down of dynamics at pH 6 from ~250 fs to ~600 fs upon addition of NaCl.[12] This was explained by screening of the static interfacial electric field and hence of the vSFG probing depth due to the presence of counterions at the interface.[12] Thus, the vibrational dynamics of water next to the silica surface was observed to be sensitive to both surface charge and ionic strength.[10,12]

The vibrational lifetime of the O—H stretch at the Al_2O_3(0001)/H_2O interface also depends on the bulk pH (Figure 3 and Table 1). At positively and negatively charged alumina surfaces (pH 2−4 and pH 10−12 respectively), the vibrational lifetime is short (T_1 = 100−125 fs), but at the neutral alumina (0001) surface (pH 6), the vibrational lifetime is two times longer (T_1 = ~ 220 fs). This is in contrast to the vibrational dynamics observed in our previous study[31] at the $Al_2O_3(11\bar{2}0)$/H_2O interface (Figure 4) where the T_1 lifetime

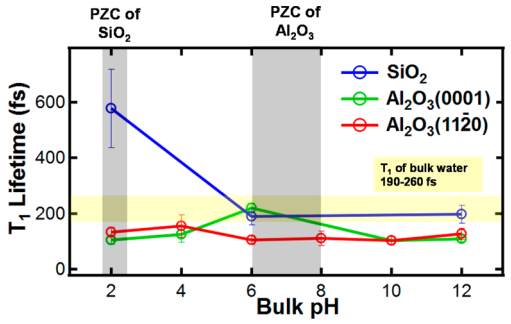

Figure 4. Effect of surface charge (pH 2−12) on T_1, the vibrational lifetime of the interfacial OH species, at the SiO_2/H_2O interface (blue),[10] the α-$Al_2O_3(11\bar{2}0)$/H_2O interface (red),[31] and the α-Al_2O_3(0001)/H_2O interface (green). The shaded gray areas represent the PZC of SiO_2 and Al_2O_3 surfaces. The shaded yellow region represents the range of reported T_1 lifetimes of bulk water.

was always short (T_1 = 100−155 fs) and the dynamics did not slow down even at pH 6 bulk solution (PZC of alumina). This result is consistent with the vSFG results (Figure 2) discussed earlier where we observed that the 3000 cm^{-1} species is absent or smaller at the α-Al_2O_3(0001)/H_2O interface compared to the α-$Al_2O_3(11\bar{2}0)$/H_2O interface for pH 6 bulk solution. This suggests that the 3000 cm^{-1} species observed at the alumina/water interface plays an important role in the fast (T_1 = ~100 fs) vibrational dynamics and in its absence (pH 6 at the α-Al_2O_3(0001)/H_2O interface) the vibrational relaxation slows down (T_1 = ~220 fs). Additionally, the faster relaxation of water next to the neutral $Al_2O_3(11\bar{2}0)$ surface (pH 6 bulk solution) provides further evidence that the water next to the $(11\bar{2}0)$ surface is "more ordered and strongly hydrogen bonded" than the (0001) surface, as predicted by Catalano.[3,37]

In comparison to the silica surface, the vibrational dynamics of water next to alumina surfaces is distinctly different (Figure 4). First of all, the T_1 of O—H stretch at the neutral Al_2O_3(0001) surface (pH 6 bulk solution) is almost three times smaller than at the neutral SiO_2 surface (pH 2 bulk solution) where the interfacial water molecules are incompletely solvated (1 Si—OH: 5 H—OH, as discussed earlier) and hence display slow vibrational dynamics due to inefficient vibrational energy transfer.[10] In contrast, at the neutral alumina(0001) surface, the interfacial water molecules are more completely solvated (1 Al—OH: 1 H—OH) and, therefore, display fast and bulk water-like vibrational dynamics in contrast to what is observed at the charged silica/water interface. In addition, it is clear that the T_1 lifetime of the O—H stretch at the charged alumina surface (~100 fs) is shorter than at the charged silica surface and bulk water (~200 fs). Only at pH 6 for the Al_2O_3(0001)/H_2O interface does the T_1 lifetime reduce to ~200 fs. This observation further suggests that the 3000 cm^{-1} species, which is prominent at the charged α-Al_2O_3(0001)/H_2O interface, plays a key role in the fast vibrational dynamics (T_1 = ~ 100 fs) because in the absence of the 3000 cm^{-1} species (at pH 6 for the Al_2O_3(0001) surface), the vibrational dynamics is slower (T_1 = ~ 200 fs).

The next obvious question is why the vibrational dynamics of water next to a charged Al_2O_3(0001) surface is faster than at the charged silica surface or even bulk water? From our results discussed earlier, it is clear that the low frequency O—H stretches (~3000 cm^{-1}) play a prominent role. DFT calculations from our previous study[31] on the α-$Al_2O_3(11\bar{2}0)$/H_2O interface revealed that proton transfer is prominent between associated and dissociated water molecules at the interface. Another MD simulation study[27] on thin water films adsorbed on the α-Al_2O_3(0001) surface also revealed formation of different kinds of associated and dissociated water molecules generated via proton transfer reactions. Additionally, a time-resolved infrared study proposed that the vibrational relaxation of the O—H stretch at the γ-Al_2O_3/air interface was due to photoinduced proton transfer from the surface aluminol groups to neighboring water molecules adsorbed from the ambient air.[30] The excited state proton transfer reaction in water is very fast (~100 fs)[30,52] and it is possible that the vibrational relaxation at the alumina/water interface is dominated by a proton transfer reaction. The increase of the T_1 lifetime at pH 6 for the Al_2O_3(0001)/H_2O interface also supports proton transfer as a viable mechanism of vibrational relaxation since at neutral pH (neat water), the alumina surface is net neutral and most of the aluminol groups exist as neutral Al—OH and therefore the proton transfer reaction is less probable. On the contrary, at acidic and basic bulk pHs, the alumina surface is positively and negatively charged, respectively, and a large number of aluminol groups exist as Al—

DOI: 10.1021/acs.jpcc.7b00499
J. Phys. Chem. C 2017, 121, 5168−5177

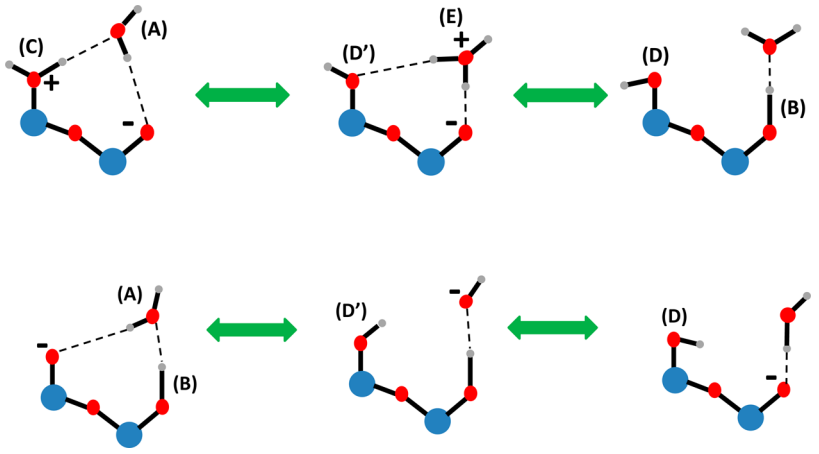

Figure 5. Schemes of possible proton transfer reactions at the α-$Al_2O_3(0001)/H_2O$ interface at acidic pH (top panel) and at basic pH (bottom panel).[27] The blue, red and gray spheres represent aluminum, oxygen, and hydrogen atoms, respectively. (A–E) represent different types of OH groups present at the interface. In acidic pH, the C species initially transfers a proton to a nearby water molecule (A) which forms a hydronium ion (E) leaving behind D′, which slightly changes orientation to form D. The hydronium ion (E) then transfers a proton to a nearby oxygen atom of the mineral lattice to form a new OH species (B). In basic pH, the negatively charged Al—O^- species initially receives a proton from a nearby water molecule (A) to form a neutral D species. The water molecule converts into a negatively charged hydroxyl group, which receives a proton from nearby neutral aluminol groups (B). Adapted from ref 27.

OH_2^+ and Al—O^- which are critical players in the proton transfer reaction (Figure 5). Consequently, the proton transfer reaction should be prominent at charged alumina surfaces (acidic and basic bulk pH) and could cause the vibrational dynamics to be faster than that in bulk water.

It is important to understand how proton transfer reactions between different O—H stretches at the $Al_2O_3(0001)/H_2O$ interface can affect the vibrational dynamics time scales. As mentioned earlier, the assignment of the vSFG spectra of the $Al_2O_3(0001)/H_2O$ interface is not straightforward as there are O—H stretches from both aluminol groups and interfacial water molecules, which was also observed in a recent MD simulation study of a thin water film adsorbed on the $Al_2O_3(0001)$ surface.[27] The different types of O—H stretches at the $Al_2O_3(0001)/H_2O$ interface include:

A. strongly hydrogen bonded physisorbed water;
B. strongly hydrogen bonded surface aluminol groups (dissociated chemisorbed water);
C. strongly hydrogen bonded associated chemisorbed water;
D. non-hydrogen bonded surface aluminol groups; and
E. hydronium ion (in acidic pH) or OH^- (in basic solutions)

The theoretical study showed that in the presence of water, the alumina (0001) surface is gradually hydroxylated via proton transfer reactions between the different OH groups present in the interfacial region (Figure 5).[27]

In our IR pump-vSFG probe experiments (that excite and interrogate the 2900–3300 cm^{-1} region), we are not exclusively pumping and probing one kind of OH species. All the strongly hydrogen bonded OH groups are probed simultaneously and hence can contribute to the vSFG signal. We speculate that the excited state proton transfer reaction dominates the vibrational relaxation via the following mechanism (Figure 6). For simplicity, let us assume that only the strongly hydrogen bonded aluminol group (C species, Figure 6, top) is pumped and probed. At time zero, the intense pump IR excites the C species from the vibrational ground state ($\nu = 0$) to the first excited state ($\nu = 1$) causing a bleach of the probe vSFG signal, which means that there is a decrease in the population of the C species in the vibrational ground state. The recovery of the bleach can be due to two processes: (a) the excited C species ($\nu = 1$) relaxing back to the ground state ($\nu = 0$) via energy transfer, or (b) the formation of a new species whose frequency is within the probe IR window (2900–3300 cm^{-1}). As shown in the above scheme (Figure 5), the proton transfer reaction can cause the C species to convert into a D species, and in the process form a new B species. The observed recovery of the bleach can be due to the formation of the B species, whose spectral frequency is within the vSFG probe window. In this mechanism, the species responsible for the bleach (the C species) and the species responsible for the recovery of the bleach (the B species) are different. However, since the vSFG probe window is broad, it is also pumping and probing other strongly hydrogen bonded OH species, e.g., the A species (Figure 6, bottom). The initial bleach can also be due to exciting the A species from the ground state ($\nu = 0$) to the first excited state ($\nu = 1$). During the proton transfer reaction, the A species receives a proton from the C species to form the hydronium ion (the E species). The proton is then transferred from the hydronium ion (E species) to the oxygen atom of the alumina surface to form the B species. Upon doing so, the hydronium ion is converted back to the A species (which is oriented differently from the initial A species) and we expect the O—H stretch of the new A species not to be in the excited state anymore. Therefore, the formation of the ground state A species causes the recovery of the bleach. In this scenario, the species responsible for the bleach and the recovery of the bleach is the same. Proton transfer reactions involving both the A and the C species are probably involved in the ultrafast vibrational relaxation pathway. The proton transfer reaction can also form a D species, which is non-hydrogen bonded and therefore highly blue-shifted (and outside the vSFG probe region). Since the time scale of excited state proton transfer is reported to be ~100 fs, which is in agreement with our T_1 relaxation time scales, we speculate that the faster than bulk-water vibrational relaxation observed in this study could be due to an excited state proton transfer reaction between different OH species present at the $Al_2O_3(0001)/H_2O$ interface.

DOI: 10.1021/acs.jpcc.7b00499
J. Phys. Chem. C 2017, 121, 5168–5177

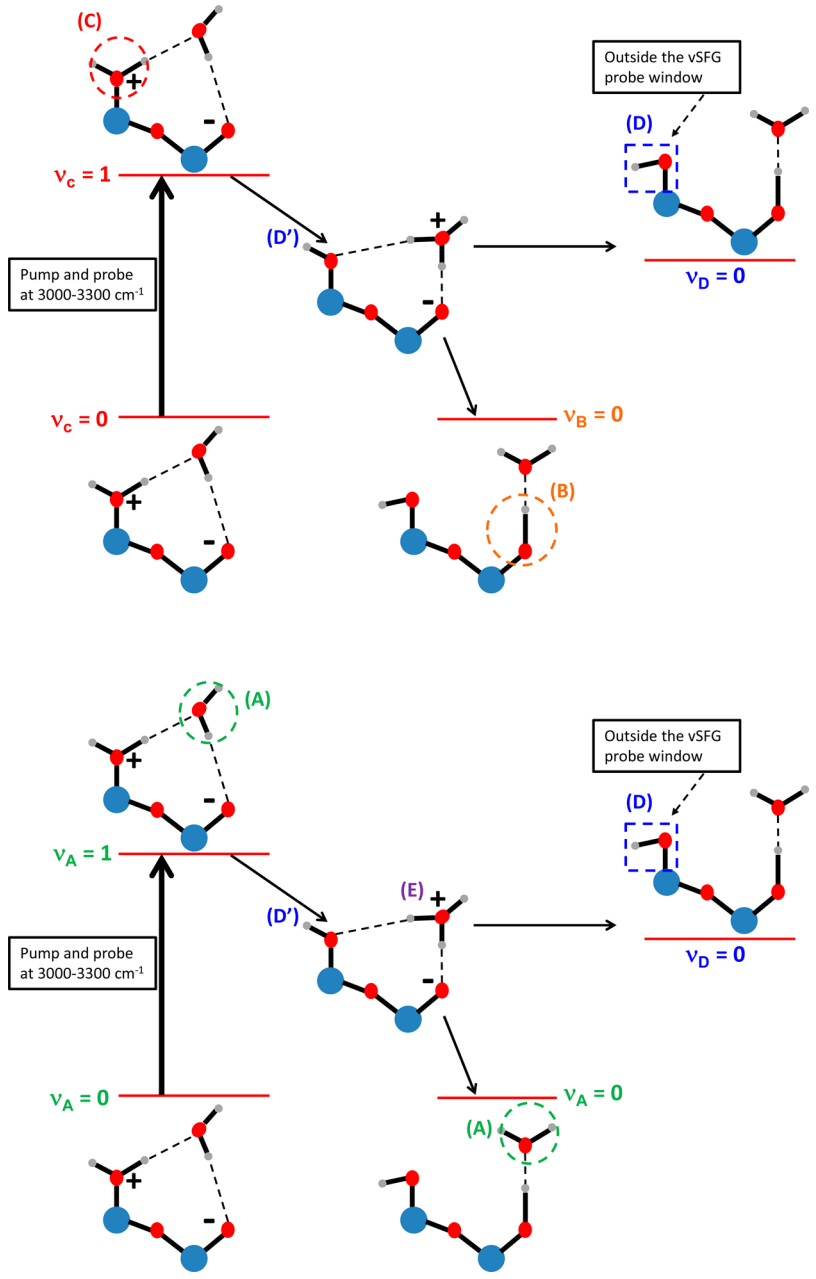

Figure 6. Schemes of the possible mechanisms and pathways of vibrational relaxation via an ultrafast excited state proton transfer reaction between the different OH groups present at the α-$Al_2O_3(0001)/H_2O$ interface. The top panel shows the vibrational relaxation pathway involving the C species and the B species, whereas the bottom panel shows the vibrational relaxation pathway involving the A species. The dashed circles represent different OH species responsible for the initial bleach and the recovery of the bleach. The dashed squares represent the OH species which do not contribute to the vibrational relaxation pathway since they lie outside the vSFG probe. Cartoons adapted from ref 27.

Alternatively, the observation that the vibrational dynamics of the O—H stretches at the Al_2O_3/H_2O interface are faster than in bulk water can also be explained by a better coupling between the O—H stretch and the H_2O bend due to the presence of low frequency (~3000 cm^{-1}) OH species at the Al_2O_3/H_2O interface. A similar argument has been suggested to explain why the OH vibrational dynamics in ice is faster than in liquid water.[51] At the positively and negatively charged alumina/water interfaces, the 3000 cm^{-1} species is prominent in the vSFG spectra (Figure 1 and 2). The presence of 3000 cm^{-1} species allows for a better coupling between the O—H stretch and the H_2O bend overtone, which in turn allows for an efficient pathway for the vibrational relaxation. However, at the neutral $Al_2O_3(0001)/H_2O$ interface, the 3000 cm^{-1} species is barely observed in the vSFG spectra (Figure 1 and 2) and hence the vibrational relaxation slows down so that it resembles bulk water-like dynamics. Consistent with this picture, since the 3000 cm^{-1} species is still prominent at pH 6–8 for the $Al_2O_3(11\bar{2}0)/H_2O$ interface, in contrast to the neutral $Al_2O_3(0001)/H_2O$ interface, the vibrational dynamics remains faster than in bulk water.

We have also investigated the effect of excess ions (0.1 M NaCl) on the time scale of vibrational relaxation at the $Al_2O_3(0001)/H_2O$ interface (Figure 7). Similar to the $Al_2O_3(11\bar{2}0)/H_2O$ interface, the addition of excess ions has little to no effect on the vibrational dynamics of the O—H

DOI: 10.1021/acs.jpcc.7b00499
J. Phys. Chem. C 2017, 121, 5168–5177

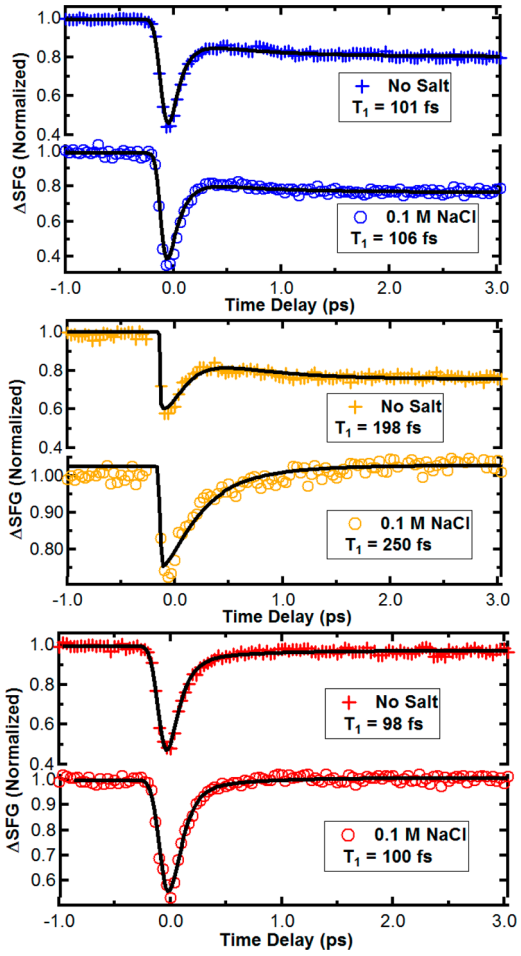

Figure 7. Effect of ions (0.1 M NaCl) on the vibrational relaxation dynamics of the interfacial OH species at the α-$Al_2O_3(0001)/H_2O$ interface for bulk pH 2 (blue), pH 6 (yellow), and pH 12 (red). The "+" symbols represent data where no excess salt is added and the "O" symbols represent data where 0.1 M NaCl is added. The solid lines are the best fits consistent with a four-level system (described in the SI). P-polarized IR pump and PPP-polarized vSFG probe were used.

stretches at the $Al_2O_3(0001)/H_2O$ interface, i.e., for either the positively or the negatively charged surfaces (pH 2 and pH 12, respectively), the vibrational dynamics is faster than in bulk water ($T_1 \approx 100$ fs) either with or without excess ions. Similarly, at the PZC (pH 6), excess ions only slightly affect the T_1 time scale. This is in contrast to the large effect of ions observed at the silica surface.[12] This result suggests that the presence of excess ions is able to change the interfacial water structure next to the silica surface such that the rate or the mechanism of vibrational relaxation of excited O—H stretches is altered. However, excess ions are not able to change the interfacial water structure next to the alumina surface sufficiently to alter the rate of vibrational relaxation of excited O—H stretches. This contrasting salt effect seems to suggest two things: (a) the mechanism of vibrational relaxation at the alumina/water interface is different from the silica/water interface and hence the salt effects are different, and/or, (b) hydrogen bonding environment at the alumina/water interface is stronger than at the silica/water interface so that the counterions at the alumina/water interface cannot alter the hydrogen bonding network of the interfacial region sufficiently to affect its ultrafast vibrational dynamics.

In conclusion, we have investigated the structure and the dynamics of the $Al_2O_3(0001)$/water interface using steady-state and time-resolved vSFG spectroscopy. The vSFG spectra of the O—H stretch reveals that "the $Al_2O_3(0001)$ surface is less ordered and weakly hydrogen bonded than the $Al_2O_3(11\bar{2}0)$ surface".[3,37] Additionally, the vibrational dynamics of the O—H stretch of the charged alumina/water interface is faster than in bulk water and at a charged silica surface, which could be due to ultrafast excited state proton transfer reaction and/or better coupling between the O—H stretch and the H_2O bend overtone via the presence of low frequency (red-shifted) OH species. While both of the proposed reasons as to why the vibrational dynamics at the alumina/water interface is faster than that in bulk water seem reasonable, our experiments are not able to provide definitive evidence in support of one mechanism over the other. Lastly, the contrasting excess salt effect on the vibrational dynamics of interfacial water next to alumina and silica surfaces seems to agree with the view that the mechanism of vibrational relaxation at the two distinct mineral surfaces could be different and/or the interfacial hydrogen bonding network of interfacial water next to the alumina surface is stronger than that at the silica surface.

■ ASSOCIATED CONTENT

Supporting Information

The Supporting Information is available free of charge on the ACS Publications website at DOI: 10.1021/acs.jpcc.7b00499.

Fitting of the IR pump-vSFG probe data using a 4 level model is briefly discussed. Effect of the IR pump power and the IR polarization on the vibrational dynamics of the O—H stretch at the $Al_2O_3(0001)/H_2O$ interface is discussed (PDF)

■ AUTHOR INFORMATION

Corresponding Author

*E-mail: eborguet@temple.edu.

Notes

The authors declare no competing financial interest.

■ ACKNOWLEDGMENTS

The authors acknowledge the National Science Foundation for supporting this work (NSF Grant CHE 1337880). The authors thank Professor M. Zdilla (Temple University, Chemistry Department) for alumina prism face orientation identification by X-ray diffraction and Dr. Kyle Gilroy (Professor S. Neretina Group, Temple University, College of Engineering) for gold coating of the alumina prisms.

■ REFERENCES

(1) Henderson, M. A. The Interaction of Water With Solid Surfaces: Fundamental Aspects Revisited. *Surf. Sci. Rep.* **2002**, *46*, 1−308.

(2) Kelber, J. A. Alumina Surfaces and Interfaces Under Non-Ultrahigh Vacuum Conditions. *Surf. Sci. Rep.* **2007**, *62*, 271−303.

(3) Catalano, J. G. Weak Interfacial Water Ordering on Isostructural Hematite and Corundum (001) Surfaces. *Geochim. Cosmochim. Acta* **2011**, *75*, 2062−2071.

(4) Du, Q.; Freysz, E.; Shen, Y. R. Vibrational Spectra of Water Molecules at Quartz/Water Interfaces. *Phys. Rev. Lett.* **1994**, *72*, 238−241.

(5) Ong, S.; Zhao, X.; Eisenthal, K. B. Polarization of Water Molecules at a Charged Interface: Second Harmonic Studies of the Silica/Water Interface. *Chem. Phys. Lett.* **1992**, *191*, 327−335.

DOI: 10.1021/acs.jpcc.7b00499
J. Phys. Chem. C 2017, 121, 5168−5177

(6) Zhang, L.; Tian, C.; Waychunas, G. A.; Shen, Y. R. Structures and Charging of α-Alumina (0001)/Water Interfaces Studied by Sum-Frequency Vibrational Spectroscopy. *J. Am. Chem. Soc.* **2008**, *130*, 7686−7694.
(7) Yeganeh, M.; Dougal, S.; Pink, H. Vibrational Spectroscopy of Water at Liquid/Solid Interfaces: Crossing the Isoelectric Point of a Solid Surface. *Phys. Rev. Lett.* **1999**, *83*, 1179.
(8) Dewan, S.; Yeganeh, M. S.; Borguet, E. Experimental Correlation Between Interfacial Water Structure and Mineral Reactivity. *J. Phys. Chem. Lett.* **2013**, *4*, 1977−1982.
(9) Yang, Z.; Li, Q.; Chou, K. C. Structures of Water Molecules at the Interfaces of Aqueous Salt Solutions and Silica: Cation Effects. *J. Phys. Chem. C* **2009**, *113*, 8201−8205.
(10) Eftekhari-Bafrooei, A.; Borguet, E. Effect of Surface Charge on the Vibrational Dynamics of Interfacial Water. *J. Am. Chem. Soc.* **2009**, *131*, 12034−12035.
(11) Eftekhari-Bafrooei, A.; Borguet, E. Effect of Hydrogen-Bond Strength on the Vibrational Relaxation of Interfacial Water. *J. Am. Chem. Soc.* **2010**, *132*, 3756−3761.
(12) Eftekhari-Bafrooei, A.; Borguet, E. Effect of Electric Fields on the Ultrafast Vibrational Relaxation of Water at a Charged Solid−Liquid Interface as Probed by Vibrational Sum Frequency Generation. *J. Phys. Chem. Lett.* **2011**, *2*, 1353−1358.
(13) Ostroverkhov, V.; Waychunas, G. A.; Shen, Y. Vibrational Spectra of Water at Water/α-Quartz (0001) Interface. *Chem. Phys. Lett.* **2004**, *386*, 144−148.
(14) Azam, M. S.; Weeraman, C. N.; Gibbs-Davis, J. M. Specific Cation Effects on the Bimodal Acid−Base Behavior of the Silica/Water Interface. *J. Phys. Chem. Lett.* **2012**, *3*, 1269−1274.
(15) Dewan, S.; Carnevale, V.; Bankura, A.; Eftekhari-Bafrooei, A.; Fiorin, G.; Klein, M. L.; Borguet, E. Structure of Water at Charged Interfaces: A Molecular Dynamics Study. *Langmuir* **2014**, *30*, 8056−8065.
(16) Jena, K. C.; Covert, P. A.; Hore, D. K. The Effect of Salt on the Water Structure at a Charged Solid Surface: Differentiating Second- and Third-order Nonlinear Contributions. *J. Phys. Chem. Lett.* **2011**, *2*, 1056−1061.
(17) Sulpizi, M.; Gaigeot, M. P.; Sprik, M. The Silica-Water Interface: How the Silanols Determine the Surface Acidity and Modulate the Water Properties. *J. Chem. Theory Comput.* **2012**, *8*, 1037−1047.
(18) Pfeiffer-Laplaud, M.; Costa, D.; Tielens, F.; Gaigeot, M. P.; Sulpizi, M. Bimodal Acidity at the Amorphous Silica/Water Interface. *J. Phys. Chem. C* **2015**, *119*, 27354−27362.
(19) Pfeiffer-Laplaud, M.; Gaigeot, M.-P. Electrolytes at the Hydroxylated (0001) α-Quartz/Water Interface: Location and Structural Effects on Interfacial Silanols by DFT-Based MD. *J. Phys. Chem. C* **2016**, *120*, 14034.
(20) Pfeiffer-Laplaud, M.; Gaigeot, M. P. Adsorption of Singly Charged Ions at the Hydroxylated (0001) alpha-Quartz/Water Interface. *J. Phys. Chem. C* **2016**, *120*, 4866−4880.
(21) Isaienko, O.; Borguet, E. Hydrophobicity of Hydroxylated Amorphous Fused Silica Surfaces. *Langmuir* **2013**, *29*, 7885−7895.
(22) Ostroverkhov, V.; Waychunas, G. A.; Shen, Y. R. New Information on Water Interfacial Structure Revealed by Phase-Sensitive Surface Spectroscopy. *Phys. Rev. Lett.* **2005**, *94*, 4.
(23) Sovago, M.; Campen, R. K.; Wurpel, G. W. H.; Muller, M.; Bakker, H. J.; Bonn, M. Vibrational Response of Hydrogen-Bonded Interfacial Water is Dominated by Intramolecular Coupling. *Phys. Rev. Lett.* **2008**, *100*, 100.
(24) Myalitsin, A.; Urashima, S. H.; Nihonyanagi, S.; Yamaguchi, S.; Tahara, T. Water Structure at the Buried Silica/Aqueous Interface Studied by Heterodyne-Detected Vibrational Sum-Frequency Generation. *J. Phys. Chem. C* **2016**, *120*, 9357−9363.
(25) Baumgarten, E.; Wagner, R.; Lentes-Wagner, C. Quantitative Determination of Hydroxyl Groups on Alumina by IR Spectroscopy. *Anal. Bioanal. Chem.* **1989**, *334*, 246−251.
(26) Hass, K. C.; Schneider, W. F.; Curioni, A.; Andreoni, W. The Chemistry of Water on Alumina Surfaces: Reaction Dynamics from First Principles. *Science* **1998**, *282*, 265−268.
(27) Ma, S. Y.; Liu, L. M.; Wang, S. Q. Water Film Adsorbed on the alpha-Al_2O_3(0001) Surface: Structural Properties and Dynamical Behaviors from First-Principles Molecular Dynamics Simulations. *J. Phys. Chem. C* **2016**, *120*, 5398−5409.
(28) Huang, P.; Pham, T. A.; Galli, G.; Schwegler, E. Alumina (0001)/Water Interface: Structural Properties and Infrared Spectra from First-Principles Molecular Dynamics Simulations. *J. Phys. Chem. C* **2014**, *118*, 8944−8951.
(29) Gaigeot, M. P.; Sprik, M.; Sulpizi, M. Oxide/Water Interfaces: How the Surface Chemistry Modifies Interfacial Water Properties. *J. Phys.: Condens. Matter* **2012**, *24*, 11.
(30) Le Caër, S.; Palmer, D. J.; Lima, M.; Renault, J. P.; Vigneron, G.; Righini, R.; Pommeret, S. Time-Resolved Studies of Water Dynamics and Proton Transfer at the Alumina-Air Interface. *J. Am. Chem. Soc.* **2007**, *129*, 11720−11729.
(31) Tuladhar, A.; Dewan, S.; Kubicki, J. D.; Borguet, E. Spectroscopy and Ultrafast Vibrational Dynamics of Strongly Hydrogen Bonded OH Species at the α-Al_2O_3(11−20)/H_2O Interface. *J. Phys. Chem. C* **2016**, *120*, 1615310.1021/acs.jpcc.5b12486.
(32) Sung, J.; Shen, Y.; Waychunas, G. The Interfacial Structure of Water/Protonated α-Al_2O_3 (11−20) as a Function of pH. *J. Phys.: Condens. Matter* **2012**, *24*, 124101.
(33) Sung, J.; Zhang, L.; Tian, C.; Shen, Y. R.; Waychunas, G. A. Effect of pH on the Water/α-Al_2O_3 (1102) Interface Structure Studied by Sum-Frequency Vibrational Spectroscopy. *J. Phys. Chem. C* **2011**, *115*, 13887−13893.
(34) Florsheimer, M.; Kruse, K.; Polly, R.; Abdelmonem, A.; Schimmelpfennig, B.; Klenze, R.; Fanghänel, T. Hydration of Mineral Surfaces Probed at the Molecular Level. *Langmuir* **2008**, *24*, 13434−13439.
(35) Nanjundiah, K.; Hsu, P. Y.; Dhinojwala, A. Understanding Rubber Friction in the Presence of Water Using Sum-Frequency Generation Spectroscopy. *J. Chem. Phys.* **2009**, *130*, 024702.
(36) Chandrasekharan, R.; Zhang, L.; Ostroverkhov, V.; Prakash, S.; Wu, Y.; Shen, Y.-R.; Shannon, M. A. High-Temperature Hydroxylation of Alumina Crystalline Surfaces. *Surf. Sci.* **2008**, *602*, 1466−1474.
(37) Catalano, J. G. Relaxations and Interfacial Water Ordering at the Corundum (110) Surface. *J. Phys. Chem. C* **2010**, *114*, 6624−6630.
(38) Braunschweig, B.; Eissner, S.; Daum, W. Molecular Structure of a Mineral/Water Interface: Effects of Surface NanoRoughness of α-Al_2O_3(0001). *J. Phys. Chem. C* **2008**, *112*, 1751−1754.
(39) Zhuravlev, L. The Surface Chemistry of Amorphous Silica. Zhuravlev Model. *Colloids Surf., A* **2000**, *173*, 1−38.
(40) McGuire, J. A.; Shen, Y. R. Ultrafast Vibrational Dynamics at Water Interfaces. *Science* **2006**, *313*, 1945−1948.
(41) Bonn, M.; Bakker, H. J.; Ghosh, A.; Yamamoto, S.; Sovago, M.; Campen, R. K. Structural Inhomogeneity of Interfacial Water at Lipid Monolayers Revealed by Surface-Specific Vibrational Pump-Probe Spectroscopy. *J. Am. Chem. Soc.* **2010**, *132*, 14971−14978.
(42) Nihonyanagi, S.; Singh, P. C.; Yamaguchi, S.; Tahara, T. Ultrafast Vibrational Dynamics of a Charged Aqueous Interface by Femtosecond Time-Resolved Heterodyne-Detected Vibrational Sum Frequency Generation. *Bull. Chem. Soc. Jpn.* **2012**, *85*, 758−760.
(43) Nihonyanagi, S.; Mondal, J. A.; Yamaguchi, S.; Tahara, T. Structure and Dynamics of Interfacial Water Studied by Heterodyne-Detected Vibrational Sum-Frequency Generation. *Annu. Rev. Phys. Chem.* **2013**, *64*, 579−603.
(44) Ghosh, A.; Smits, M.; Sovago, M.; Bredenbeck, J.; Muller, M.; Bonn, M. Ultrafast vibrational dynamics of interfacial water. *Chem. Phys.* **2008**, *350*, 23−30.
(45) Lock, A. J.; Woutersen, S.; Bakker, H. J. Ultrafast Energy Equilibration in Hydrogen-Bonded Liquids. *J. Phys. Chem. A* **2001**, *105*, 1238−1243.
(46) Lock, A.; Bakker, H. Temperature Dependence of Vibrational Relaxation in Liquid H_2O. *J. Chem. Phys.* **2002**, *117*, 1708−1713.
(47) Kropman, M. F.; Bakker, H. J. Effect of Ions on the Vibrational Relaxation of Liquid Water. *J. Am. Chem. Soc.* **2004**, *126*, 9135−9141.

DOI: 10.1021/acs.jpcc.7b00499
J. Phys. Chem. C 2017, 121, 5168−5177

(48) Lindner, J.; Vöhringer, P.; Pshenichnikov, M. S.; Cringus, D.; Wiersma, D. A.; Mostovoy, M. Vibrational Relaxation of Pure Liquid Water. *Chem. Phys. Lett.* **2006**, *421*, 329−333.
(49) Ashihara, S.; Huse, N.; Espagne, A.; Nibbering, E. T. J.; Elsaesser, T. Ultrafast Structural Dynamics of Water Induced by Dissipation of Vibrational Energy. *J. Phys. Chem. A* **2007**, *111*, 743−746.
(50) Bakker, H.; Skinner, J. Vibrational Spectroscopy as a Probe of Structure and Dynamics in Liquid Water. *Chem. Rev.* **2010**, *110*, 1498−1517.
(51) Woutersen, S.; Emmerichs, U.; Nienhuys, H.-K.; Bakker, H. J. Anomalous Temperature Dependence of Vibrational Lifetimes in Water and Ice. *Phys. Rev. Lett.* **1998**, *81*, 1106−1109.
(52) Simkovitch, R.; Karton-Lifshin, N.; Shomer, S.; Shabat, D.; Huppert, D. Ultrafast Excited-State Proton Transfer to the Solvent Occurs on a Hundred-Femtosecond Time-Scale. *J. Phys. Chem. A* **2013**, *117*, 3405−3413.

DOI: 10.1021/acs.jpcc.7b00499
J. Phys. Chem. C 2017, 121, 5168−5177